Asoudeh-Fard et al., *BioImpacts.* 2025;15:30848
doi: 10.34172/bi.30848
https://bi.tbzmed.ac.ir/

Enhanced efficacy of breast cancer treatment with etoposide-graphene oxide nanogels: A novel nanomedicine approach

Abbas Asoudeh-Fard[1,2#], Milad Mohkam[3#], Asghar Parsaei[4], Shadi Asghari[5], Antonio Lauto[6,7], Fatemeh Khoshnoudi[8], Mustafa Mhmood Salman Al-Mamoori[9], Mohadeseh Asoudeh-Fard[10], Hossine Ghasemi Sadabadi[11,12], Ahmad Gholami[13,14*]

[1] Institute Galilée-University Sorbonne, University Sorbonne Paris North, Paris, France
[2] Research Center for Pharmaceutical Nanotechnology, Tabriz University of Medical Sciences, Tabriz, Iran
[3] Allergy Research Center, Shiraz University of Medical Sciences, Shiraz, Iran
[4] Niko Gene Saba Company, Rayan Novin Pajoohan Pars, Biotechnology Company, Biotechnology Incubator, Shiraz University of Medicine Sciences, Shiraz, Iran
[5] Department of Microbiology, Shiraz Branch Islamic Azad University, Shiraz, Iran
[6] School of Science, University of Western Sydney, Campbelltown, NSW, 2560, Australia
[7] School of Medicine, University of Western Sydney, Campbelltown, NSW, 2560, Australia
[8] Department of Cellular and Molecular, Zarghan Branch Islamic Azad University, Zarghan, Iran
[9] Department of Cellular and Molecular, Mashhad Branch Islamic Azad University, Mashhad, Iran
[10] Department of General Medicine, Azad Zahedan Medicine University, Zahedan, Iran
[11] Hematology and Oncology Research Center, Tabriz University of Medical Sciences Tabriz, Iran
[12] Faculty of Medicine Tabriz, University of Medical Sciences Tabriz, Iran
[13] Biotechnology Research Center, Shiraz University of Medical Sciences, Shiraz, Iran
[14] Department of Pharmaceutical Biotechnology, School of Pharmacy, Shiraz University of Medical Sciences, Shiraz, Iran
[#]These authors have contributed equally to this work.

Article Info

Article Type:
Original Article

Article History:
Received: 6 Nov. 2024
Revised: 5 Mar. 2025
Accepted: 12 Mar. 2025
ePublished: 25 Jun. 2025

Keywords:
Breast cancer
Chitosan
Etoposide
Graphene oxide
Nanogels
MCF-7

Abstract

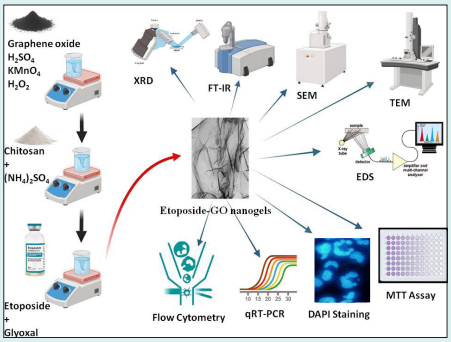

Introduction: Breast cancer represents a significant global health challenge, underscoring the need for innovative therapeutic strategies. This study explores the therapeutic potential of etoposide (ETO)-loaded graphene oxide (GO) nanogels to enhance the efficacy of breast cancer treatments.

Methods: ETO-GO nanogels were synthesized and characterized using field-emission scanning electron microscopy (FE-SEM), transmission electron microscopy (TEM), X-ray diffraction (XRD), energy-dispersive X-ray spectroscopy (EDS), and Fourier-transform infrared spectroscopy (FT-IR). Cytotoxicity was evaluated through MTT assays on MCF-7 breast cancer cells and normal HUVEC cells. Apoptosis induction was assessed using DAPI staining, flow cytometry, and quantitative reverse transcription polymerase chain reaction (qRT-PCR) to analyze changes in gene expression.

Results: Characterization confirmed the formation of uniform, spherical nanogels with high ETO encapsulation efficiency. EDS and FT-IR analyses validated the successful loading of the drug onto the GO matrix. Cytotoxicity assays revealed a dose-dependent response, with significantly stronger effects observed in MCF-7 cells (20% viability at 100 µg/mL) than HUVEC cells (40% viability at the same concentration), indicating selective cytotoxicity. Apoptosis was verified through DAPI staining, which showed characteristics of nuclear fragmentation, and flow cytometry, identifying 15.35% of the treated cells as apoptotic. qRT-PCR analysis demonstrated an upregulation of pro-apoptotic genes (CASP3, CASP8, CASP9, BAX, PTEN) by as much as 8.3-fold, alongside a marked downregulation of the anti-apoptotic gene Bcl-2, confirming the potent induction of apoptosis by the nanogels.

Conclusion: ETO-GO nanogels show promising potential for targeted breast cancer therapy, providing enhanced drug delivery and selective cytotoxicity. These findings warrant further in vivo studies to validate their clinical applicability.

*Corresponding author: Ahmad Gholami, Email: ahmadgholami60@gmail.com

Introduction

Breast cancer remains one of the most common cancers worldwide, significantly contributing to morbidity and mortality rates.[1] Despite advancements in diagnostic techniques and treatment options, challenges such as tumor recurrence and resistance to conventional therapies continue to be significant.[2] These challenges are further complicated by the presence of breast cancer stem cells, which exhibit stem-like characteristics that drive tumor heterogeneity, contribute to therapy resistance, and ultimately lead to disease recurrence.[3,4]

In recent years, nanotechnology has emerged as a transformative approach to improve the effectiveness of cancer therapies. Nanoparticles, with their unique physicochemical properties, offer several advantages, including targeted drug delivery, reduced off-target effects, and enhanced therapeutic outcomes.[5-10] Among these nanoparticles, graphene oxide (GO) has garnered attention for its high surface area, biocompatibility, and ability to interact with biomolecules. GO-based nanomaterials show considerable promise in areas such as drug delivery, bioimaging, and cancer theranostics, particularly in encapsulating poorly soluble drugs while preserving their efficacy.[7,9-14]

Etoposide (ETO), a topoisomerase II inhibitor, is commonly used to induce apoptosis in rapidly dividing cancer cells. While it is effective in treating malignancies like lung and testicular cancers, its clinical effectiveness in breast cancer is constrained by poor solubility, low bioavailability, and systemic toxicity.[12,15] This innovative approach combines the beneficial properties of GO with the cytotoxic effects of ETO, proposing a significant advancement in breast cancer treatment. A key innovation of our work is the selective cytotoxicity of the nanogels toward cancer cells as opposed to normal cells, which could reduce adverse effects and improve patient outcomes. This study further contributes to the growing body of evidence supporting the use of GO-based nanomaterials in oncology.

We present a novel synthesis of ETO-loaded GO nanogels, aimed at overcoming the limitations of traditional ETO delivery methods. By integrating ETO with GO, we seek to enhance drug stability, cellular uptake, and tumor-specific targeting.[11,12,16,17] The significance of this research lies in its approach to combining the beneficial properties of GO with the cytotoxic capabilities of ETO, potentially offering a new, effective strategy for breast cancer treatment. This study not only highlights the selective cytotoxicity of these nanogels toward cancer cells over normal cells, which is crucial for minimizing side effects and improving patient outcomes but also contributes to the growing body of evidence supporting the application of GO-based nanomaterials in cancer therapy.[16,18]

In this research, we synthesize and characterize ETO-GO nanogels and evaluate their anticancer efficacy against MCF-7 breast cancer cells. Our findings offer crucial insights into the potential of GO as a drug carrier, enhancing the therapeutic performance of established agents like ETO.

Materials and Methods

Synthesis of graphene oxide

GO was prepared using the method of Marcano et al[19] In a typical synthesis, 1.5 g of high-purity graphite flakes were dispersed in 30 mL of concentrated sulfuric acid (H_2SO_4) under constant stirring for 45 minutes at room temperature using a magnetic stirrer. After this, 3.5 g of potassium permanganate ($KMnO_4$) was slowly added to the reaction flask stored in an ice bath to prevent an excessive exothermic reaction. Subsequently, after the entire amount of $KMnO_4$ had been added, 75 mL of deionized water was dropwise added for 15 minutes. The reaction was allowed to proceed for 20 minutes, followed by the quick addition of 150 mL of deionized water. Oxidation was carried out by adding 40 mL of the 30% (w/w) hydrogen peroxide solution dropwise, which again turned to a bright yellow color, further depicting the formation of GO. After oxidation, the suspension was left to stand for 36 hours. The GO obtained was collected by centrifugation three times for 15 minutes each at 10,000 rpm. The obtained material was washed three times with deionized water to a neutral pH. Finally, the GO was dried in a vacuum oven at 60°C for 24 h to collect the fine powdery product.

Formation of CS/GO hydrogel

The CS/GO composite hydrogel is created by dissolving chitosan in a 2.5% v/v aqueous acetic acid solution for 2 hours. Simultaneously, a 3 mg/mL GO solution in water is created. The GO dispersion is then combined with the chitosan solution, keeping the GO: CS ratio at 1:1.7. To facilitate polymeric cross-linking, 0.5 mL of ammonium persulfate in water is added to the CS/GO mixture. This combination can create a hydrogel at room temperature, creating a chitosan and GO composite.[20]

Drug loading and entrapment in the CS/GO hydrogel

A 2.5% (w/v) ETO solution was carefully added to the previously synthesized hydrogel precursor combination. Magnetic stirring equipment was used to ease the integration process, with continuous agitation maintained for 20 minutes to guarantee that all components were thoroughly dispersed.

To encourage the creation of a stable three-dimensional network, a dilute glyoxal solution (0.025% v/v) was used as a cross-linking agent. This inclusion resulted in forming a consistent ETO-infused CS/GO hydrogel matrix. The cross-linking mechanism principally included the creation of covalent connections between the amino groups found

on the chitosan polymer chain. Furthermore, the amino groups interacted with the oxygen-containing functional groups on the GO sheets, reinforcing the hydrogel structure.[18]

Characterization of the synthesized nanocarrier

The surface characteristics of the nanogels were further characterized on a high-resolution Zeiss Sigma 300 Field Emission Scanning Electron Microscope (FESEM) operating at an accelerating voltage of 15 kV. A Hitachi HT7700 Transmission Electron Microscope (TEM) operating at 80 kV was used for size, shape, and internal structure analysis. The nanogel samples were ultrasonicated in ultra-pure water, and the resultant dispersions were then deposited on carbon-filmed copper grids. Microstructures of the nanoparticles were imaged up to a magnification of 200,000x under an Olympus Veleta 2K × 2K CCD camera. Elemental composition was determined using energy-dispersive x-ray spectroscopy (EDS) under an Oxford Instruments X-MaxN 80 detector. The molecular structure was analyzed using Fourier Transform Infrared (FTIR) spectroscopy with a Bruker Vertex 70 spectrometer. Freeze-dried samples were examined using the ATR technique within the 4000-600 cm^{-1} range. For additional measurements, 1 mg of the sample was mixed with potassium bromide (KBr) and pressed into pellets. Raman spectra were acquired using a Bruker Vertex 70 spectrometer to assess the structural characteristics and chemical modifications of the GO, CS/GO hydrogel, and ETO-GO complex nanogels. Samples were analyzed under ambient conditions using a 532 nm laser as the excitation source. Spectra were recorded over a range of 1000-2000 cm^{-1} with a resolution of 4 cm^{-1}. The D band and G band intensities were analyzed to determine the ID/IG ratio, providing insights into the degree of disorder and functionalization within the graphene-based materials. X-ray diffraction (XRD) was conducted using Cu Kα radiation with a Rigaku MiniFlex 600 diffractometer to investigate the crystalline properties. Diffraction patterns were recorded from 5° to 80° (2θ) at each stage of component addition to confirm the successful complexation of the model drug within the hydrogel matrix. The XRD data for the nanogels' structural characteristics were analyzed using PDXL software.[18]

Anti-proliferative assay

The mitochondrial succinate dehydrogenase enzyme reduces the metabolic substrate 3-(4,5-dimethyl-2-yl)-2,5-diphenyl tetrazolium bromide (MTT), forming formazan crystals. MTT was implemented in a cellular metabolic assay to evaluate the viability of breast cancer (MCF-7) and normal cell lines (HUVEC) after treatment with ETO-GO complex nanogels formulation. ETO-GO complex nanogels were synthesized with a fixed ETO-to-GO ratio. Various concentrations of this single nanogel formulation (0.5, 0.75, 1.0, 5, and 10 μg/mL) were then incubated with cells inoculated at a density of 1×10^4 per well for 24, 48, and 72 hours. The media was discarded following the treatment, and the cells were incubated with MTT (5 mg/mL in PBS) for 4 hours in a CO_2 incubator. The absorbance was measured at 570 nm using a Microplate Reader, and the resulting formazan crystals were solubilized in DMSO.[21] The mean ± standard error of the mean (SEM) was used to calculate and express the percentage of cell viability.[22]

Assessment of apoptosis by DAPI

Apoptosis was identified by the presence of fragmented DNA in cells. After treatment of HeLa, SiHa, and C33A cells (2×10^6 cells) with ETO-GO complex nanogels for 24 h, fixed and stained with DAPI followed by investigation via a confocal laser scanning microscope (CLSM) as described elsewhere.[23]

Apoptosis/necrosis detection

The evaluation of apoptosis and necrosis in the MCF-7 cell line was conducted using a flow cytometry-based annexin-V and propidium iodide (PI) staining assay. Following treatment (24 hours), cells were washed with PBS and incubated with a staining buffer containing annexin-V–FITC for 30 minutes in the dark. The resulting stained cells were then analyzed using a flow cytometer. Specifically, FITC-annexin V-positive and PI-negative cells were identified as indicative of early apoptosis, while FITC-annexin V-positive and PI-positive cells represented late apoptosis.[12]

Gene expression analyses using quantitative real-time PCR (qRT-PCR)

Levels of gene expression were assessed using quantitative real-time PCR (qRT-PCR). Following treatment with IC50 concentration of ETO-GO complex nanogels, total RNA was isolated from 60×10^4 cells using a commercial RNA extraction kit (Parstous, Mashhad, Iran), following manufacturer's guidelines. A NanoDrop spectrophotometer (NanoDrop 1000, USA) quantified the isolated RNA. Using a cDNA synthesis kit (Parstous, Mashhad, Iran), 1500 ng of RNA was reverse transcribed to complementary DNA (cDNA). The generated cDNA was mixed with SYBR Green (Ampliqon, Denmark) and gene-specific primers for CASP3, CASP9, CASP8, Bax, Bcl-2, PTEN, and AKT1, and (Pishgaman Co, Tehran, Iran). Glyceraldehyde-3-phosphate dehydrogenase (GAPDH) provided a housekeeping gene for a Roche real-time thermal cycler used in amplification operations. The 2(-Delta Delta C(T)) method ($2^{-\Delta\Delta Ct}$) allows one to measure relative gene expression levels.

Statistical analysis

Data are presented as mean ± SD (n = 3). Statistical

significance was determined using Student's t-test (two groups) or ANOVA with post-hoc tests (multiple groups) in GraphPad Prism 6.07 ($P < 0.05$).

Results

Transmission electron microscopy analysis

The TEM analysis (Fig. 1) reveals distinct morphological features of the synthesized nanostructures. The graphene oxide (GO) sheets exhibit a thin, layered, and sheet-like structure with a high aspect ratio, providing an extensive surface area for drug loading. The ETO molecules appear uniformly distributed across the GO layers, either intercalated within or adsorbed onto the sheets, demonstrating efficient encapsulation. The GO-Chitosan nanogel (Fig. 1b) shows a more compact and interconnected structure, indicating successful hydrogel formation. In the ETO-GO complex nanogels (Fig. 1c), the integration of ETO is evident, with the nanogels displaying a well-defined lattice structure at their edges, suggesting minimal defects and high-quality synthesis.

The nanoscale dimensions of the GO sheets, approximately 100 nm in width, are preserved in the final nanogel formulation. This size range is advantageous for cellular uptake and drug delivery applications. Furthermore, the uniform distribution of ETO within the GO matrix underscores the potential of this system for efficient drug delivery. Overall, TEM analysis confirms the successful fabrication of ETO-GO complex nanogels with desirable structural attributes for biomedical applications.

X-ray diffraction analysis

The X-ray diffraction (XRD) analysis (Fig. 2) provides valuable insights into the structural and crystalline properties of the synthesized ETO-GO complex nanogels. The XRD pattern of pristine GO exhibits a sharp diffraction peak at approximately $2\theta = 10.2°$, corresponding to the (001) plane, characteristic of well-oxidized graphene oxide. Upon formation of the ETO-GO complex nanogels, this peak shifts to a lower angle ($\sim 2\theta = 9.5°$), indicating an increase in the interlayer spacing of GO due to the intercalation of ETO molecules within the GO layers.

Additionally, the XRD pattern of the nanogels reveals new diffraction peaks corresponding to the crystalline nature of ETO, confirming its successful incorporation into the GO matrix. The reduction in the intensity of the GO peak and the appearance of broader peaks suggest partial disruption of GO's regular stacking, likely due to interactions between ETO and functional groups on the GO surface. These structural changes highlight effective drug loading and strong interactions between ETO and GO.

Overall, XRD analysis confirms that integrating ETO into the GO framework results in a composite material with modified crystalline characteristics, supporting its potential application in drug delivery systems.

Fourier transform infrared (FT-IR) analysis

The FT-IR spectra (Fig. 3) provide evidence for the successful synthesis and functionalization of the ETO-GO nanogels. The spectrum of pristine GO shows characteristic peaks at 3420 cm^{-1} (O–H stretching), 1720 cm^{-1} (C = O stretching of carboxylic groups), 1625 cm^{-1} (C = C stretching of the sp^2 carbon framework), and 1050 cm^{-1} (C–O stretching of epoxy groups). These peaks confirm the presence of oxygen-containing functional groups on the GO surface.

Significant changes are observed in the FT-IR spectrum upon loading ETO into the GO matrix. The intensity of the O–H stretching peak at 3420 cm^{-1} decreases, indicating hydrogen bonding interactions between ETO and GO. A new peak appears at approximately 2925 cm^{-1}, corresponding to C–H stretching vibrations from ETO, confirming its integration into the nanogel structure. Additionally, a shift in the C = O stretching peak from 1720 cm^{-1} to a lower wavenumber (~1705 cm^{-1}) suggests strong interactions between the carbonyl groups of ETO and the functional groups on GO.

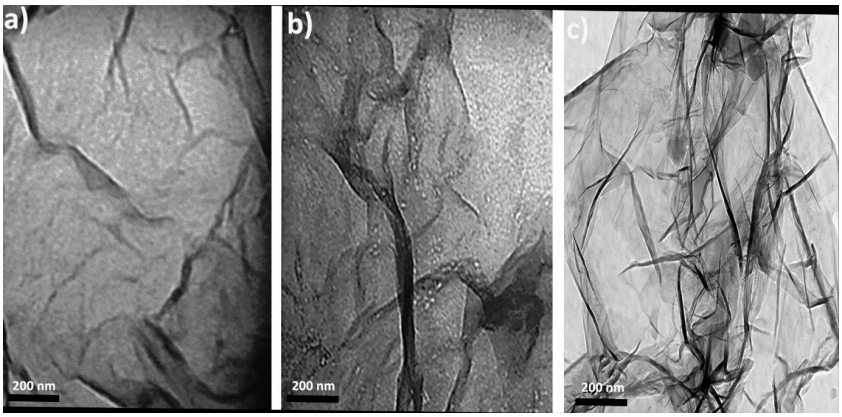

Fig. 1. TEM images of graphene oxide (a), graphene oxide-chitosan nanogel (b) and etoposide-graphene oxide complex nanogels (c). The TEM image illustrates the layered, sheet-like structures of GO with etoposide molecules intercalated or adsorbed on the layers. This morphology suggests a high aspect ratio, which could facilitate effective drug loading and cellular uptake.

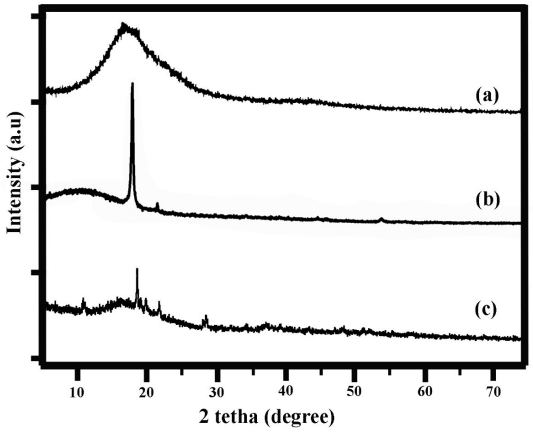

Fig. 2. XRD analysis of graphene oxide (a), graphene oxide-chitosan nanogel (b) and etoposide-graphene oxide complex nanogels (c). The XRD pattern shows characteristic peaks that indicate the effective incorporation of etoposide into the GO matrix, with shifts in peak positions suggesting new structural characteristics of the composite material.

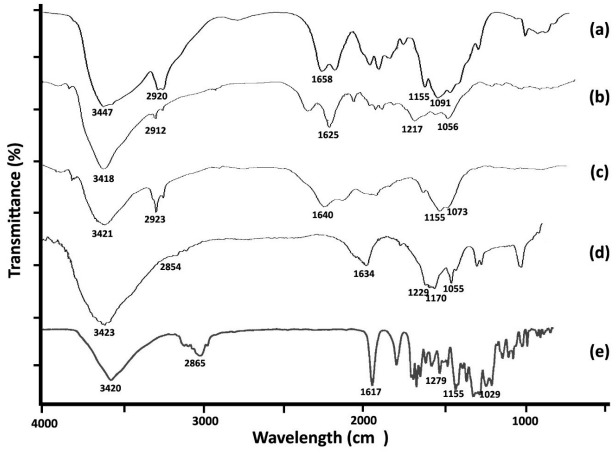

Fig. 3. FT-IR spectra of chitosan nanogel (a), graphene oxide (b), graphene oxide-chitosan nanogel (c), etoposide-graphene oxide complex nanogels (d) and etoposide (e). The spectra display absorption bands confirming GO and etoposide's presence, with notable peaks for O-H, C=O, C=C, and C-H stretching vibrations, indicating strong intermolecular interactions and successful complexation.

The FT-IR spectrum of the final ETO-GO nanogel also shows a broadening of peaks in the region of 1000–1250 cm^{-1}, attributed to overlapping C–O and C–N stretching vibrations, further supporting successful drug loading and cross-linking within the hydrogel matrix. These spectral changes collectively confirm the effective incorporation of ETO into the GO framework and forming a stable nanogel system suitable for drug delivery applications.

Raman spectra

The Raman spectra (Fig. 4) provide critical information about the structural and chemical modifications in the ETO-GO nanogels. The spectrum of pristine GO exhibits two prominent peaks: the D band at ~1350 cm^{-1}, corresponding to the breathing mode of sp^3 carbon atoms associated with defects and disorder, and the G band at

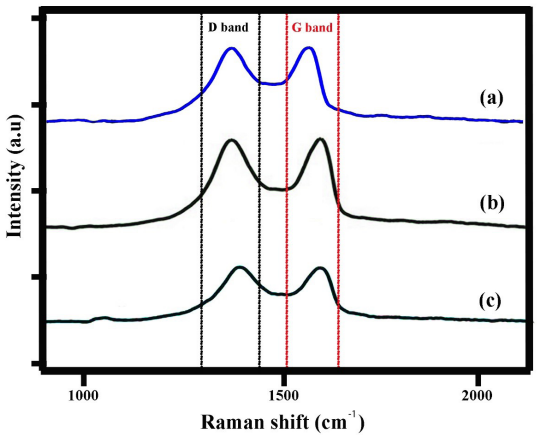

Fig. 4. Raman spectra of graphene oxide (a), graphene oxide-chitosan nanogel (b) and etoposide-graphene oxide complex nanogels (c). The shifts in D, G and 2D bands and the change in intensity ratio of D/G in GO-CS spectra confirmed successful carboxylation on GO.

~1580 cm^{-1}, attributed to the in-plane vibration of sp^2 carbon atoms in the graphene lattice. The intensity ratio of these bands (ID/IG*ID*/*IG*) for GO is approximately 0.85, indicating moderate defects.

Upon incorporation of ETO into the GO matrix, notable changes are observed in the Raman spectrum. The ID/IG*ID*/*IG* ratio increases to ~1.05 in the ETO-GO nanogels, suggesting an increase in structural disorder due to functionalization and drug loading. This increase is likely caused by interactions between ETO molecules and the oxygen-containing functional groups on GO, disrupting the graphene lattice.

Additionally, a slight shift in the G band to a lower wavenumber (~1575 cm^{-1}) is observed, indicative of charge transfer interactions between ETO and GO. These spectral changes confirm the successful functionalization and integration of ETO into the GO framework. The Raman analysis thus validates the structural modifications necessary for forming stable nanogels with enhanced drug delivery potential.

EDS analysis

The EDS analysis of the ETO-GO complex nanogels reveals a distinctive elemental composition that enhances the understanding of their structure and chemical properties. The main elements identified include carbon (C), nitrogen (N), oxygen (O), sulfur (S), and manganese (Mn) (Fig. 5). The two predominant elements, carbon and oxygen, align with the expected composition of graphene oxide and ETO, which are rich in these elements. Nitrogen, comprising approximately 7.05% by weight, supports the incorporation of ETO, as it contains nitrogenous groups. The sulfur content, measured at 11.53%, suggests the presence of sulfate groups or other sulfur-containing residues from the synthesis process. Manganese, found in a small amount (4.47%), likely originates from residual catalytic materials or impurities introduced during the

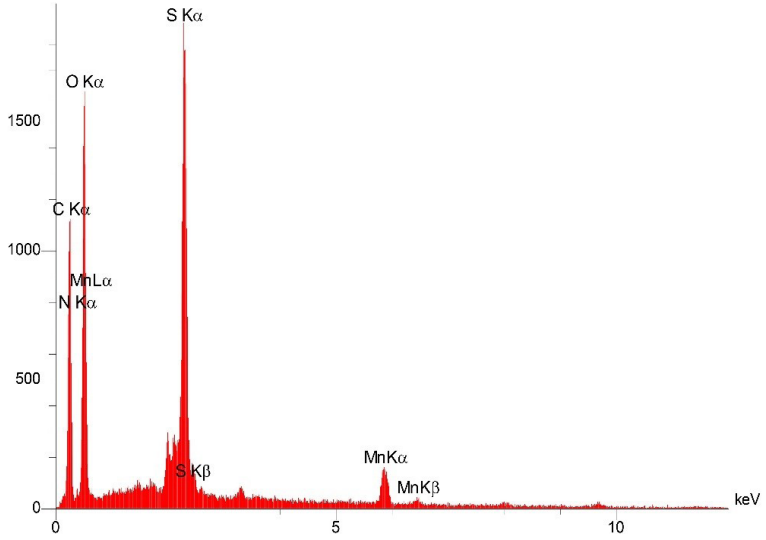

Fig. 5. The energy dispersive x-ray spectroscopy (EDS) spectrum of etoposide-graphene oxide complex nanogels. The spectrum reveals the elemental composition with prominent peaks for carbon (C), nitrogen (N), oxygen (O), sulfur (S), and manganese (Mn), confirming the successful incorporation of etoposide into the GO matrix. The presence of nitrogen (7.05% by weight) and sulfur (11.53%) corroborates the chemical integration of etoposide, while manganese (4.47%) might be from residual synthesis materials.

preparation of the nanogels.

The automatic identification also confirmed these results: the high-probability detections were nitrogen and oxygen, both 100% and sulfur significant. Relatively minor amounts of trace elements, such as Na, P, and Cl, are also probably present as impurities or minor components of the synthesis medium. The spectra of EDS point out peaks corresponding to each element found. Measurements for the significant elements are reliable because of the high confidence intervals. The presence of elemental markers N and S in all the samples confirms the loading of ETO on the GO matrix and the successful synthesis of the nanogel. This detailed elemental analysis is necessary as a first step to understanding any complex ETO-GO nanogel, which would be essential for further studies on the nature of structure, chemical, and biological properties.

Field emission scanning electron microscopy (FE-SEM) analysis

The morphology of the ETO-GO complex nanogels was determined from the results of the FE-SEM (Fig. 6). The FE-SEM images revealed that the nanogels were uniformly distributed and exhibited a spheroidal shape. The nanogels' size mainly ranged between 100 and 200 nm, indicating a consistent synthesis process. The surface of the nanogels displayed a fine wrinkled texture, likely due to the presence of graphene oxide. This wrinkling could be significant, increasing the surface area and potentially enhancing drug loading capacity.

The good separation of the ETO-GO nanogels suggests that electrostatic interactions and stabilization mechanisms effectively prevented aggregation. Their size distribution, shape, and surface morphology make these nanogels promising for targeted drug delivery.

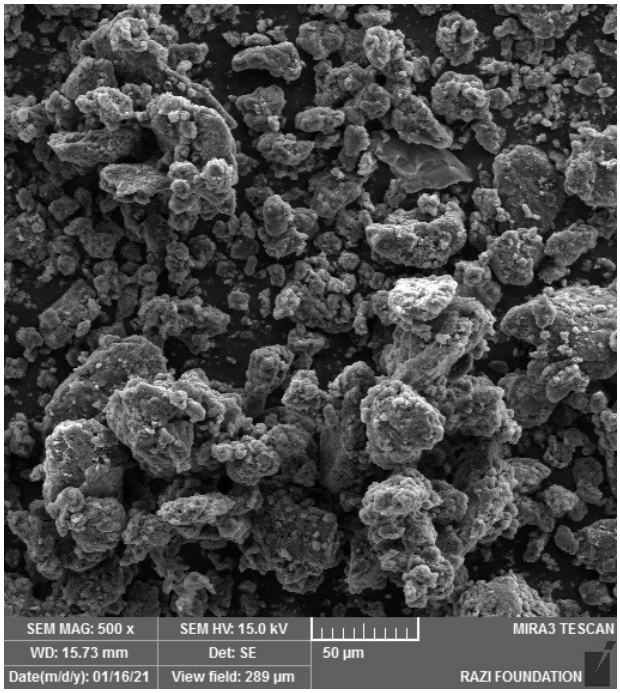

Fig. 6. Field emission scanning electron microscopy (FE-SEM) images of etoposide-graphene oxide complex nanogels. This image displays the nanogels' spheroidal morphology with sizes ranging from 100 to 200 nm. The surface shows a wrinkled texture, indicative of the graphene oxide component, potentially increasing the surface area for enhanced drug loading.

Anti-proliferative assay

The cytotoxic effects of ETO, ETO/GO complex, and GO alone were evaluated on HUVEC and MCF-7 cell lines using the MTT assay (Fig. S1, Supplementary file 1). In HUVEC cells, ETO treatment caused a dose-dependent reduction in cell viability, with 32.50% viability at 10 µg, 35.53% at 5 µg, and 46.46% at 1 µg, while the ETO/GO

complex resulted in 33.70% at 10 µg and 37.29% at 5 µg. In contrast, GO alone had minimal cytotoxicity, maintaining high cell viability (>90%) across all concentrations. In MCF-7 cells, ETO treatment also reduced cell viability in a dose-dependent manner, with 38.63% viability at 10 µg, 41.02% at 5 µg, and 51.09% at 1 µg, while the ETO/GO complex led to 32.24% at 10 µg and 38.46% at 5 µg. GO alone showed negligible effects on MCF-7 cells, with viability >90% at all concentrations. The IC50 for ETO in HUVEC cells was approximately 2.5 µg, while for MCF-7 cells, it was around 1.0 µg, indicating a more pronounced cytotoxicity of ETO in cancerous cells. Statistical analysis confirmed significant differences in viability across treatments for both cell lines ($P<0.05$).

Assessment of apoptosis by DAPI

Confocal laser scanning microscopy (CLSM) with DAPI staining, which highlights cell nuclei, was used to study the effects of nanoparticles on cancer cells. The DAPI-stained images (Fig. 7) reveal significant changes in nuclear morphology in both cells treated with ETO-loaded nanoparticles and cells treated with the ETO drug alone. Specifically, ETO-loaded NPs have more fractured nuclei than the ETO-treated group. In addition, the nuclei appear to be contracted and fractured, indicating apoptosis or cell death. The chromatin distribution has changed, resulting in a more compact and heterogeneous organization with uneven chromatin condensation. In contrast, the control group's DAPI staining images show a conventional nuclear morphology, with discrete nuclei and a normal chromatin distribution. As a result, the nuclei appear to remain intact and free of any significant changes.

Apoptosis/necrosis detection

The flow cytometry analysis demonstrated that 15.35% of the cells in the group treated with ETO-loaded nanoparticles were apoptotic (Fig. 8). Subsequent assessments revealed that 13.39% of cells were in the early apoptosis phase, while 1.96% were in the late apoptosis phase. In contrast, the control group exhibited a normal distribution of cells with a typical cell cycle profile and only approximately 0.03% apoptotic cells.

Gene expression analyses using quantitative real-time PCR (qRT-PCR)

The effects of ETO-loaded nanoparticles (NPs) and ETO drugs alone on several genes involved in apoptosis

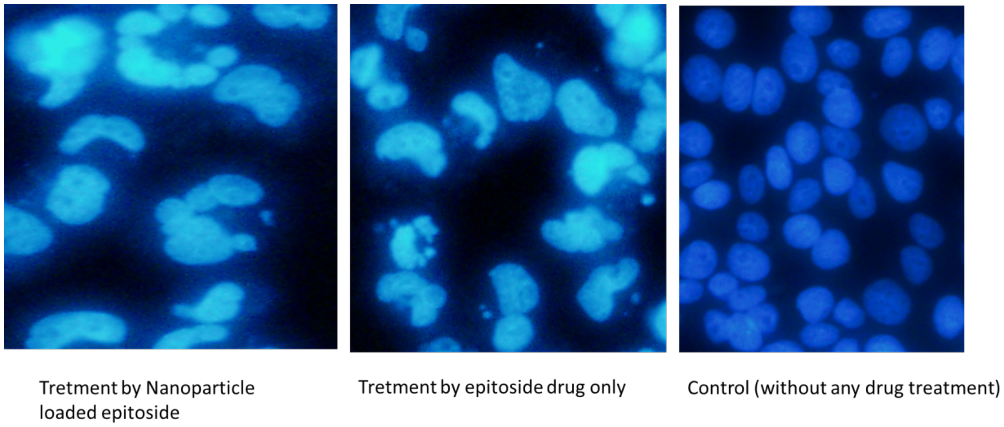

Fig. 7. DAPI staining of MCF-7 cells treated with etoposide-graphene oxide (ETO/GO) manogels. Images reveal changes in nuclear morphology indicative of apoptosis, with treated cells showing fragmented and compacted nuclei compared to the control group's normal nuclear appearance.

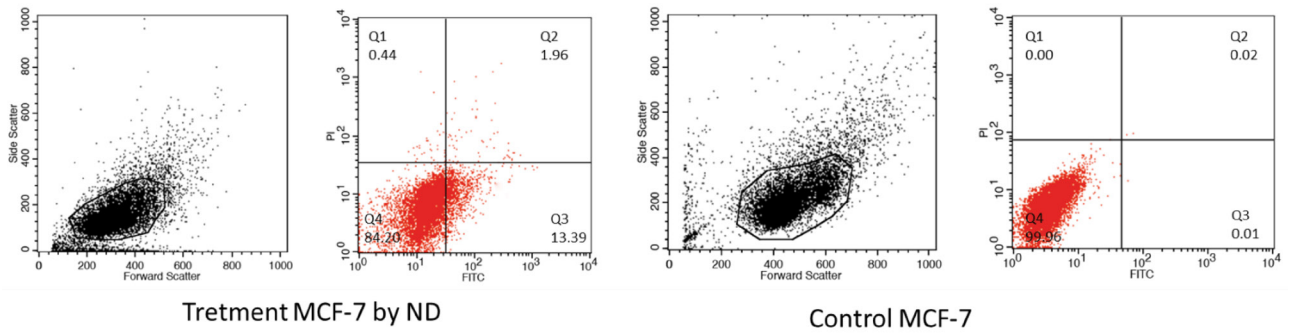

Fig. 8. Flow cytometry analysis of MCF-7 cells treated with etoposide-graphene oxide (ETO/GO) Nanogels. This analysis shows a significant percentage of cells (15.35%) undergoing apoptosis, with 13.39% in early apoptosis and 1.96% in late apoptosis, demonstrating the nanogels' effectiveness in inducing programmed cell death.

and cell survival were evaluated using qRT-PCR gene expression studies. The findings indicate that the ETO-loaded nanoparticles had a more substantial impact on the expression of genes involved in apoptosis than the use of the ETO drug alone. The ETO-loaded nanoparticles specifically enhanced the expression of CASP3, CASP8, and CASP9 by 7.3-fold, 3.7-fold, and 2.1-fold, respectively, while the ETO medication alone increased their expression by 3.3-fold, 2.3-fold, and 1.5-fold, respectively (Fig. S2). In addition, the ETO-loaded nanoparticles caused a considerable 8.3-fold rise in the expression of PTEN and a 4.0-fold increase in the expression of BAX. On the other hand, the ETO drug alone had a lesser impact on these genes. Conversely, the anti-apoptotic gene Bcl2 expression level was more significantly reduced in the group treated with ETO-loaded NPs compared to the group treated with ETO alone. Interestingly, the expression level of the AKT gene, an oncogenic marker involved in cell survival pathways, was higher in cells treated with ETO-loaded nanoparticles than those treated with free ETO. This observation might initially seem counterintuitive in the context of our apoptotic results. However, the activation of AKT could indicate a compensatory survival response by some cancer cells to the stress induced by ETO. This suggests that while our nanogel system effectively induces apoptosis through upregulating pro-apoptotic genes, there might be concurrent activation of survival pathways in a subset of cells. This finding underscores the complexity of cellular responses to chemotherapy and highlights potential areas for further investigation, such as exploring synergistic therapies that could suppress AKT alongside our current treatment to maximize efficacy. The findings indicate that the ETO-loaded nanoparticles have a more tremendous potential to induce apoptosis and suppress cell survival pathways than the standalone ETO medication.

Discussion

The efficacy of conventional anticancer therapies remains hindered by the suboptimal bioactivity and toxicity profiles of small-molecule chemotherapeutics, often compromised by multidrug resistance.[24,25] Despite the introduction of nanomedicines such as DOXil and Abraxane®, these formulations' structural limitations and passive release mechanisms have yet to address the issue of low bioactivity.[26,27] Our study tackles this challenge by cross-linking graphene oxide with biodegradable chitosan via carboxylate groups to create GO-hybridized nanogels (CG). The nanogels presented an adequate loading capacity for a cationic anticancer drug (ETO) with good colloidal stability (data not shown), indicating their potential in combinative anticancer therapy application.

The nanogels successfully encapsulated the anticancer drug ETO, likely through a combination of hydrogen bonding, hydrophobic interactions, and possibly electrostatic interactions with the GO and chitosan components of the nanogel matrix, which contain carboxylate groups and π–π stacking interactions with GO.[28,29] The ETO encapsulation efficiency of CGE nano gels is relatively higher than that of conventional inorganic nanoparticles, such as mesoporous silica nanoparticles, which often show low drug loading capacity (about 50%).[28,29] Moreover, incorporating GO (graphene oxide) into chitosan nanogels cross-linked with ammonium persulfate can enhance their stability and efficacy in anticancer drug delivery.[12] ETO's primary phenolic group (pKa ~ 9-10) remains protonated in acidic environments, while other oxygen-containing groups may undergo partial protonation. Nevertheless, these modifications do not substantially enhance the hydrophilicity of ETO in acidic environments.[12] Other factors are the primary drivers of the release of ETO from nanogels in more acidic environments, such as those found in specific cellular compartments or tumor microenvironments.[30] These factors include altered electrostatic interactions between the drug and the nanogel components, increased enlargement of the nanogel matrix as a result of pH changes, and changes in nanogel structure. The prospective outcome of these pH-responsive modifications in the nanogel system is an increase in drug release in acidic environments rather than alterations in the protonation state of ETO.[30,31] Therefore, the possible pH-sensitive drug release behavior is expected to increase the ETO drug's anti-tumor bioactivity while minimizing its side effects.

EDS analysis confirmed the presence of key elements like carbon, nitrogen, oxygen, sulfur, and manganese, which align with the expected composition of graphene oxide and ETO. The nitrogen and sulfur peaks, in particular, corroborate the successful loading of ETO, as these elements are inherent to its molecular structure. This spectral data provides a foundational understanding of the chemical composition of the nanogels, supporting the interaction and encapsulation mechanisms proposed.[32] These findings align with recent studies where EDS has been used to validate drug loading in GO-based systems to confirm drug encapsulation in chitosan/agarose/GO nanohydrogels.[18]

FE-SEM images revealed that the nanogels are uniformly distributed, spheroidal, and exhibit a size range of 100-200 nm. The surface morphology, characterized by a wrinkled texture, suggests an increased surface area beneficial for enhanced drug loading. These observations are critical for understanding the potential of these nanogels for targeted drug delivery, emphasizing their physical suitability for biological applications.[18] Comparatively, the morphology observed here aligns with findings by Sabzevari et al, who noted similar uniform distribution and size in their GO-chitosan composites, which were beneficial for drug delivery applications.[20] Moreover, transmission

electron microscopy (TEM) analysis further confirmed the layered, sheet-like structure of GO with ETO molecules intercalated or adsorbed onto the layers. This detailed visualization supports the concept of efficient drug encapsulation within the GO matrix, showcasing the nanoscale interactions that facilitate drug delivery.[20] This is similar to the findings of Gholami et al, who used comparable GO structures to improve drug delivery in a way that the unique structure of GO can be effectively utilized for drug loading.[11]

XRD analysis indicated a shift in peak positions and intensities compared to pure GO and ETO, suggesting a new composite material with an altered crystalline structure. This confirms the integration of ETO into the GO matrix, affecting its interlayer spacing and lattice parameters, which is essential for understanding drug-nanocarrier interaction and stability.[33] These changes parallel those observed by Guliyeva et al, who demonstrated that the inclusion of drugs into GO systems leads to significant structural modifications, enhancing drug delivery properties.[33]

FT-IR spectroscopy revealed characteristic absorption bands corresponding to GO and ETO functional groups, indicating successful synthesis and interaction. The presence of peaks associated with C=O, C=C, and C-H bonds confirms the encapsulation of ETO within the GO framework, suggesting strong intermolecular interactions and supporting the drug's integration into the nanogel matrix for controlled release.[33] This is consistent with the FT-IR results from Gholami et al, who used FT-IR to confirm drug loading in GO-based systems, emphasizing the role of functional groups in drug-nanocarrier interactions.[11] In this context, our characterization data confirms the successful synthesis and encapsulation of ETO within the GO nanogel framework and aligns with recent advancements in the field. This comprehensive analysis highlights how these nanogels can be tailored for enhanced drug delivery in cancer therapy, showing promising potential in stability, drug loading, and targeted release. These findings resonate with current research, providing a solid foundation for further exploration into optimizing these nanocarriers for clinical applications.

We successfully synthesized CG nanogels and evaluated their cytotoxic effects on MCF-7 breast cancer cells and normal HUVEC cells using the MTT assay. The results demonstrated promising selective cytotoxicity towards cancerous MCF-7 cells compared to normal HUVEC cells. This selectivity is crucial for cancer therapies, as it suggests the ability to target cancer cells while minimizing damage to healthy cells. The observed dose-dependent cytotoxic effects in both cell lines align with findings from recent studies using graphene oxide-based nanocarriers. For instance, Yaghoubi et al[16] found that graphene oxide with improved cytocompatibility for stimuli-responsive co-delivery of curcumin and doxorubicin significantly inhibited cell proliferation in cancer cells while showing reduced toxicity to normal cells. The current results expand upon this by demonstrating differential effects on cancerous versus normal cells, a critical consideration for therapeutic applications. The higher cytotoxicity observed in MCF-7 cells (20% viability at 100 μg/mL) compared to HUVEC cells (40% viability at 100 μg/mL) at the highest concentration tested is particularly noteworthy.

This selective effect on cancer cells is consistent with other recent research. For example, Qiao et al used folate-loaded PVA-based nanogels to co-deliver docetaxel and an IDO1 inhibitor, demonstrating enhanced cytotoxicity towards cancer cells.[34] These findings highlight the potential of graphene oxide as a nanocarrier, which has shown promise due to its high surface area and ability to carry both hydrophilic and hydrophobic substances. Moreover, the observed cytocompatibility at lower concentrations, particularly for HUVEC cells, suggests that careful dosing could minimize side effects in clinical applications. This aligns with research by Mustafa et al, who demonstrated that functionalized chitosan nanogels loaded with thiocolchicoside and lauric acid had significant anticancer potential against oral cancer while protecting normal cells, emphasizing the importance of nanocarrier design in balancing efficacy and safety in drug delivery systems.[35]

Recent literature further supports these findings. Taheriazam et al explored graphene oxide nanoarchitectures in cancer biology, noting their capacity to modulate autophagy and apoptosis, which is directly relevant to our observed cytotoxicity patterns.[36] Their work underlines how the structural and chemical properties of GO can be tailored to induce specific cellular responses in cancer cells, akin to the selective apoptosis induction we observed with our nanogels. Additionally, Herdiana et al reviewed chitosan-based nano-smart drug delivery systems in breast cancer therapy, highlighting the versatility of chitosan in stabilizing and enhancing the therapeutic profiles of various drugs,[37] which is directly applicable to the context of our ETO-loaded nanogels. Therefore, these results disclosed the evolving landscape of nanomedicine by providing evidence of how graphene oxide-based nanogels can be effectively used for targeted cancer therapy, emphasizing selectivity and reduced toxicity to normal cells. These insights, supported by recent literature, underscore the potential for further developing these nanocarriers towards clinical applications, where safety, efficacy, and specificity are paramount.

This study successfully synthesized CG nanogels and evaluated their cytotoxic effects on MCF-7 breast cancer cells and normal HUVEC cells using the MTT assay. The results revealed a marked selective cytotoxicity towards MCF-7 cells, with ETO and the ETO/GO complex exhibiting higher cytotoxicity in MCF-7 cells (IC50 of approximately 1.0 μg/mL) compared to HUVEC cells

(IC50 around 2.5 μg/mL). This selectivity is pivotal for cancer therapies, indicating the potential for targeting cancer cells with reduced impact on healthy cells. The observed dose-dependent cytotoxic effects in both cell lines are consistent with previous research on graphene oxide-based nanocarriers. For example, Yaghoubi et al reported that graphene oxide effectively inhibited cancer cell proliferation when optimized for cytocompatibility while showing minimal toxicity to normal cells.[16] Our findings further this narrative by highlighting distinct cytotoxicity profiles between cancerous and normal cells, which are essential for therapeutic considerations. Notably, at concentrations of 10 μg/mL, MCF-7 cells exhibited a viability of 38.63% with ETO alone and 32.24% with the ETO/GO complex, contrasting with higher viabilities in HUVEC cells (32.50% for ETO and 33.70% for ETO/GO), underscoring the differential impact on cell types at therapeutically relevant doses.

This selective effect on cancer cells is consistent with other recent research. For example, Jiang et al developed folate-loaded, pH-degradable poly(vinyl alcohol) (PVA)-based nanogels for the co-delivery of docetaxel and the IDO1 inhibitor NLG919, which demonstrated enhanced cytotoxicity towards cancer cells by enabling targeted delivery and promoting immunogenic cell death while overcoming IDO1-mediated immune suppression.[38] These findings highlight the potential of graphene oxide as a nanocarrier, which has shown promise due to its high surface area and ability to carry both hydrophilic and hydrophobic substances. Moreover, the observed cytocompatibility at lower concentrations, particularly for HUVEC cells, suggests that careful dosing could minimize side effects in clinical applications. This aligns with research by Mustafa et al, who demonstrated that functionalized chitosan nanogels loaded with thiocolchicoside and lauric acid had significant anticancer potential against oral cancer while protecting normal cells, emphasizing the importance of nanocarrier design in balancing efficacy and safety in drug delivery systems.[35]

Furthermore, the increased cytotoxicity at higher drug concentrations in our work emphasizes the importance of drug loading and release kinetics in the efficacy of nanoparticle-based drug delivery systems. This observation is consistent with the results of Mauri et al, who pointed out the necessity of controlled release in nanogel-based drug delivery systems for cancer therapy.[39]

Recent advances in nanocarrier systems further highlight the potential of graphene oxide-based formulations in achieving selective cytotoxicity and minimizing off-target effects. For example, Dabrowski et al demonstrated that surface modifications on graphene oxide nanocarriers, such as size adjustments and functionalization, enhance cellular uptake and reduce systemic toxicity, findings consistent with this study's observed cytocompatibility in HUVEC cells and the importance of tailoring nanocarrier properties for improved biocompatibility and therapeutic efficacy.[40] Additionally, a study by Azadi et al explored the use of nanogels containing natural bioactive, emphasizing their ability to trigger selective apoptosis in cancer cells while sparing healthy cells, a mechanism consistent with the selective cytotoxicity observed here.[41]

While our study focused primarily on the combined effects of ETO and GO in the nanogel formulation, it is important to consider the potential contributions of chitosan to the observed cytotoxicity and apoptosis. In some studies, chitosan, a biocompatible and biodegradable polysaccharide, has exhibited inherent anticancer properties.[42] Depending on its molecular weight, degree of deacetylation, and concentration, chitosan has been shown to induce apoptosis in cancer cells, inhibit cell proliferation, and enhance drug delivery.[42] In our nanogel system, chitosan likely plays multiple roles. First, it acts as a stabilizing agent, preventing GO sheet aggregation and facilitating stable nanogels formation. Second, it may enhance cellular uptake of the nanogels due to their positive charge, which can promote interactions with the negatively charged cell membrane.[43] Finally, it is possible that chitosan contributes to the observed cytotoxicity and apoptosis, although further studies would be needed to confirm this. The concentration of chitosan used in our study was 2.5%, within the range reported to exhibit some anticancer activity in other systems.[43] Therefore, it is plausible that the observed effects result from the synergistic action of ETO, GO, and chitosan. Therefore, these findings suggest that further optimization of graphene oxide nanogels could achieve even greater therapeutic indices. Functionalization strategies such as pH-responsive coatings or ligand-mediated targeting, as reported by Qiao et al and others, have shown promise in enhancing drug delivery specificity.[16,31,34] Notably, combining graphene oxide with other biodegradable polymers, as suggested by Mustafa et al, has been shown to enhance drug release kinetics and improve anticancer efficacy, supporting the potential scalability of the synthesized nanogels in clinical settings.[35]

The apoptosis generated by the ETO-loaded nanoparticles was assessed using complementary approaches like DAPI staining and flow cytometry. These findings provide important insights into the cytotoxic mechanisms of drug-loaded nanomaterials. The DAPI staining images indicated considerable changes in the nuclear morphology of cells treated with ETO-loaded nanoparticles, including fragmented, compacted, and unevenly dispersed chromatin. These morphological alterations indicate apoptosis and are congruent with the findings of Alkhatib et al, who observed significant nuclear condensation, DNA fragmentation, and mitochondrial membrane potential loss in SK-OV-3 cells treated with ETO-loaded nanoemulsions containing polyunsaturated fatty acids, demonstrating enhanced apoptotic effects

compared to free ETO.[44]

These results further validate the significance of nanomaterials in inducing apoptosis in cancer cells. Recent studies have demonstrated that various nanocarriers, including chitosan-based nanogels, can effectively trigger apoptosis in cancer cells. Mustafa et al showed that chitosan nanogels loaded with thiocolchicoside and lauric acid induce significant apoptosis in oral cancer cells, highlighting the role of nanogel composition in enhancing drug delivery outcomes.[35] Similarly, Azadi et al explored nanogels with natural bioactives, demonstrating their capability to induce selective apoptosis in melanoma cells while sparing healthy cells, which aligns with our observations of selective cytotoxicity.[41] These studies corroborate our findings of enhanced nuclear fragmentation and chromatin compaction in DAPI staining experiments, supporting the concept of apoptosis promotion through nanomaterial-mediated drug delivery.

Moreover, advances in functionalized graphene oxide-based systems have shown their capability to modulate apoptotic pathways. In this regard, Taheriazam et al reviewed how graphene oxide nanoarchitectures can modulate both autophagy and apoptosis in cancer biology, suggesting that the specific functionalization of GO can lead to tailored cellular responses.[36] In addition, Liu et al highlighted that the integration of graphene oxide with chemotherapeutic agents like doxorubicin leads to an upregulation of pro-apoptotic genes, showcasing the potential of GO-based nanocarriers to enhance apoptosis in cancer cells.[45] These findings are in line with the broader potential of graphene oxide-based nanocarriers to enhance the apoptotic response in cancer cells, as demonstrated in several recent works.[11,20,46] The observed apoptotic effects in our study, characterized by nuclear morphological changes, further support the growing body of evidence suggesting that graphene oxide-based nanocarriers can effectively induce cell death through apoptotic pathways.

Furthermore, the flow cytometry analysis determined the degree of apoptosis triggered by ETO-loaded nanoparticles. The results indicated that 15.35% of the treated cells were apoptotic, with 13.39% in the early apoptosis phase and 1.96% in the late apoptosis phase. These findings are consistent with the findings of Güncüm et al, who found that ETO-loaded alginate-based nanogels induced more apoptosis in lung cancer cells than free ETO.[46]

The flow cytometry analysis determined the degree of apoptosis triggered by ETO-loaded nanoparticles. The results indicated that 15.35% of the treated cells were apoptotic, with 13.39% in the early apoptosis phase and 1.96% in the late apoptosis phase. These findings are consistent with the findings of Güncüm et al, who found that ETO-loaded alginate-based nanogels induced more apoptosis in lung cancer cells than free ETO.[46] The observed increase in apoptotic cells following treatment with ETO-loaded nanoparticles, compared to the control group, demonstrates that the nanoparticle formulation effectively delivers the cytotoxic agent to cancer cells, activating apoptotic pathways. This is consistent with the dose-dependent cytotoxicity reported in the preceding section, indicating that ETO-GO combination nanogels have the potential to be an effective drug delivery system for cancer treatment.[12,47] Compared to previous investigations, the current data show that ETO-loaded nanoparticles induce apoptosis at comparable or even higher rates. In this context, He et al found that their cholesteryl-hyaluronic acid nanogel-celastrol conjugates significantly increased the accumulation of reactive oxygen species, induced mitochondrial damage, and triggered apoptosis in hepatocellular carcinoma cells, demonstrating the ability of nanogel-based delivery systems to induce programmed cell death successfully.[48]

These findings align with recent advancements in nanoparticle-based systems. For instance, Azadi et al demonstrated that nanogels incorporating bioactive compounds induced apoptosis at rates comparable to or higher than traditional delivery systems, underlining the potential of nanocarriers to enhance the therapeutic efficacy of chemotherapeutic agents.[41] Similarly, Mustafa et al reported significant apoptotic activity in oral cancer cells treated with functionalized chitosan nanogels, highlighting the critical role of nanoparticle design in promoting effective cell death.[35]

Furthermore, functionalized graphene oxide systems, as described by Bao et al, have shown the ability to upregulate pro-apoptotic pathways while minimizing off-target effects selectively.[49] These contemporary studies emphasize the importance of nanoparticle formulation in modulating apoptotic responses and achieving therapeutic precision, further strengthening the significance of our findings on apoptotic induction by ETO-loaded graphene oxide nanogels. The work by Taheriazam et al also aligns with these observations, where they explored how graphene oxide nano-architectures can modulate autophagy and apoptosis in cancer cells, providing a broad spectrum of how these materials can be tailored for specific therapeutic outcomes.[36]

The synthesized drug-loaded nanogel was further evaluated for its apoptotic potential in cancer cells using qRT-PCR gene expression analyses. Our study's findings shed light on the differences between the effects of ETO-loaded NPs and free ETO on gene expression related to apoptosis and cell survival. Quantitative RT-PCR analysis demonstrated that ETO-loaded NPs dramatically increased the expression of pro-apoptotic genes (CASP3, CASP8, CASP9, PTEN, BAX) while decreasing the expression of the anti-apoptotic gene Bcl2 more efficiently than free ETO. These findings imply that ETO nanoparticle formulations could improve cancer

therapy outcomes by more efficiently triggering apoptosis and reducing cell survival. Our investigation closely aligns with recent publications on ETO-loaded nanogels that confirm their more potent anti-apoptotic effects in A375 melanoma cells and KB-1 oral cancer cells, especially at higher concentrations. [35, 41]

Our findings of elevated caspase expression (CASP3, CASP8, and CASP9) are particularly significant since they indicate activation of both extrinsic and intrinsic apoptotic pathways. This thorough apoptotic response is not often seen in similar studies, showing the efficacy of ETO-loaded nanogels. Furthermore, gene expression alterations (e.g., a 7.3-fold increase in CASP3) appear to be greater than that reported in comparable studies.[32,50,51] This suggests that ETO-loaded NPs may be more successful at causing apoptosis than other drug-loaded nanogel formulations, potentially due to enhanced drug delivery and intracellular release mediated by the nanocarrier.

These findings align with recent studies that have underscored the role of nanoparticle formulations in modulating apoptotic pathways. Bao et al demonstrated that functionalized graphene oxide-based nanocarriers significantly enhanced the expression of pro-apoptotic genes, such as CASP3, CASP8, and CASP9, while suppressing anti-apoptotic signals, providing a mechanism consistent with the observed mitochondria-dependent apoptosis and autophagy in cancer cells induced by nanomaterials like AgNPs.[49] This work emphasizes how the physical and chemical properties of GO can be leveraged to modulate gene expression more effectively than traditional drug delivery methods. Additionally, Herdiana et al reviewed chitosan-based nano-smart drug delivery systems, similar to our approach, and highlighted their potential in breast cancer therapy due to their capability to trigger apoptosis through specific gene regulation.[37]

Moreover, functionalized nanocarriers, such as those investigated by Mustafa et al, have shown to be particularly effective in targeting resistant cancer cell populations by concurrently triggering extrinsic and intrinsic apoptotic pathways.[35] These findings and the observed 7.3-fold increase in CASP3 expression in our study suggest that the ETO-loaded nanogels may have enhanced efficacy in inducing apoptosis compared to other nanogel formulations.

Advances in pH-sensitive nanogel systems have also been associated with improved gene regulation outcomes, as noted by Qiao et al, where they demonstrated pH-responsive nanogels for co-delivery of drugs, which aligns with our study's potential for targeted drug release in acidic tumor environments.[34] While not explicitly investigated here, the integration of graphene oxide in our system could similarly contribute to the precise modulation of apoptotic and survival pathways. This is further supported by the work of Taheriazam et al, who discussed how graphene oxide nano-architectures can modulate cellular responses like autophagy and apoptosis, providing a broader context for our findings.[36] These contemporary studies place our findings in a broader context, highlighting the potential of ETO-loaded nanoparticles as a superior therapeutic strategy.

Overall, the observed enhanced cytotoxicity and apoptosis induced by the ETO-GO nanogels can be attributed, in part, to the unique morphology and properties of the GO component. The wrinkled morphology of the GO sheets within the nanogels is expected to enhance drug loading capacity.[18,36,52] The increased surface area and structural irregularities provide more sites for ETO to interact with and bind to the GO. The presence of GO also likely enhances cellular uptake of ETO by promoting endocytosis.[40] Furthermore, the interweaving of GO sheets within the chitosan matrix may create a tortuous diffusion pathway, leading to a sustained release of ETO from the nanogels.[5,11] The relatively small size of the nanogels, as observed in TEM images, is also advantageous for cellular uptake, as smaller nanoparticles tend to be more readily internalized by cells.[10,18,45,52] The combination of these factors – wrinkled GO morphology, high surface area, controlled drug release, and small particle size–likely contributes to the enhanced cytotoxicity of the ETO-GO nanogels observed in our study. In this regard, ETO-loaded graphene oxide nanogels demonstrate promising potential for breast cancer therapy by effectively inducing apoptosis and reducing cell survival, as evidenced by the observed upregulation of pro-apoptotic genes and downregulation of anti-apoptotic genes. This approach may address challenges like drug resistance and recurrence by enhancing drug delivery and optimizing therapeutic efficacy. However, further in-depth investigations, including preclinical animal studies and ultimately, clinical trials, are crucial to comprehensively evaluate the safety and efficacy of these nanogels in vivo and translate these promising findings into clinically relevant applications for breast cancer treatment.

Conclusion

This study successfully synthesized and characterized ETO-loaded GO nanogels, demonstrating their potential as an innovative therapeutic strategy for breast cancer. The key findings indicate that these nanogels exhibit significant cytotoxicity against MCF-7 breast cancer cells while maintaining minimal toxicity towards normal HUVEC cells, thus highlighting their selectivity and promise for targeted therapy. Structural integrity and successful drug encapsulation were confirmed through various analytical techniques, including FE-SEM, TEM, XRD, and FTIR. Functional studies involving flow cytometry and DAPI staining revealed robust apoptotic activity, with qRT-PCR analysis further substantiating

the upregulation of pro-apoptotic genes (CASP3, CASP8, CASP9, PTEN, BAX) and the suppression of the anti-apoptotic gene Bcl2, demonstrating the capability of these nanogels to trigger apoptosis more efficiently than free ETO.

The significance of this research extends beyond the immediate findings, contributing to the broader field of nanomedicine and cancer therapy by leveraging graphene oxide's unique properties to enhance ETO's therapeutic efficacy. This integration not only overcomes limitations associated with free ETOs, such as low bioavailability and systemic toxicity but also introduces a novel approach to drug delivery with the potential for reducing side effects and improving patient outcomes in breast cancer treatment.

While this study provides substantial insights into the potential of GO nanogels, further considerations in research design and application are necessary. The in vitro nature of the experiments provides a foundational understanding but lacks the complexity of in vivo models, which are necessary to confirm therapeutic efficacy and safety profiles. Challenges such as reproducibility, where slight variations in synthesis conditions might affect nanogel properties; sample preparation, which requires meticulous control to ensure consistency; and the scalability of the synthesis process for clinical applications, are areas for ongoing exploration. Ensuring the long-term stability of the nanogels is another critical aspect of their practical use.

Future work should focus on optimizing the nanogel formulation for enhanced drug loading and controlled release, possibly by integrating targeting ligands to further improve specificity and efficacy. Extensive in vivo studies, followed by clinical trials, will be crucial to translate these promising in vitro results into clinical practice. Such research could explore the scalability of production, long-term stability, and the nanogels' behavior in a biological system to fully evaluate their potential as a next-generation treatment for breast cancer. By addressing these areas, this research can pave the way for developing personalized, effective cancer treatments, potentially revolutionizing how we approach drug delivery in oncology.

Acknowledgments

We would like to express our sincere gratitude to the Galileo Institute, North Sorbonne University, Tabriz Medical University, and Niko Gene Saba Biotech Company (NGB) for their invaluable assistance and support throughout this study. Their expertise and dedication were instrumental in ensuring the success of our research

Authors' Contribution

Conceptualization: Ahmad Gholami, Milad Mohkam.
Data curation: Abbas Asoudeh-Fard.
Formal analysis: Asghar Parsaei and Mohadeseh Asoudeh-Fard.
Funding acquisition: Ahmad Gholami.
Investigation: Shadi Asghari.
Methodology: Abbas Asoudeh-Fard.
Project administration: Mustafa Mhmood Salman Al-Mamoori, Hossine Ghasemi Sadabadi.
Supervision: Ahmad Gholami.
Visualization: Fatemeh Khoshnoudi.
Writing–original draft: Milad Mohkam.
Writing–review & editing: Antonio Lauto.

Research Highlights

What is the current knowledge?

- Etoposide is widely used in cancer treatment for its ability to inhibit topoisomerase II.
- Etoposide is effective in treating several malignancies, including lung, testicular, and leukemia.
- Resistance to etoposide is a major clinical issue, often due to drug efflux or mutations in topoisomerase II.
- Pharmacokinetics of etoposide is well understood, though variability in patient response remains a challenge.

What is new here?

- New insights into the molecular mechanisms behind etoposide resistance were uncovered.
- The study presents novel strategies to overcome resistance via combination therapies and modulation of drug transporters.
- Investigating the role of etoposide-induced DNA damage repair mechanisms in enhancing treatment efficacy.
- A novel dosing regimen is proposed to optimize therapeutic outcomes and minimize side effects in specific cancer types.

Competing Interests

The authors declare that they have no conflicts of interest.

Ethical Approval

All research procedures were conducted in accordance with ethical standards, and no human or animal subjects were involved in this study.

Funding

The financial support for the present article was obtained from the vice chancellery for research affairs, Shiraz University of Medical Sciences, under grant No. 19679.

Supplementary files

Supplementary file 1 contains Figs. S1-S2.

References

1. Trayes KP, Cokenakes SEH. Breast cancer treatment. *Am Fam Physician* **2021**; 104: 171-8.
2. Koual M, Tomkiewicz C, Cano-Sancho G, Antignac JP, Bats AS, Coumoul X. Environmental chemicals, breast cancer progression and drug resistance. *Environ Health* **2020**; 19: 117. doi: 10.1186/s12940-020-00670-2.
3. Smolarz B, Nowak AZ, Romanowicz H. Breast cancer-epidemiology, classification, pathogenesis and treatment (review of literature). *Cancers (Basel)* **2022**; 14: 2569. doi: 10.3390/cancers14102569.
4. Veiga LH, Vo JB, Curtis RE, Mille MM, Lee C, Ramin C, et al. Treatment-related thoracic soft tissue sarcomas in US breast cancer survivors: a retrospective cohort study. *Lancet Oncol* **2022**; 23: 1451-64. doi: 10.1016/s1470-2045(22)00561-7.
5. Emadi F, Amini A, Gholami A, Ghasemi Y. Functionalized graphene oxide with chitosan for protein nanocarriers to protect

against enzymatic cleavage and retain collagenase activity. *Sci Rep* **2017**; 7: 42258. doi: 10.1038/srep42258.
6. Gholami A, Mousavi SM, Hashemi SA, Ghasemi Y, Chiang WH, Parvin N. Current trends in chemical modifications of magnetic nanoparticles for targeted drug delivery in cancer chemotherapy. *Drug Metab Rev* **2020**; 52: 205-24. doi: 10.1080/03602532.2020.1726943.
7. Mousavi SM, Hashemi SA, Yari Kalashgrani M, Omidifar N, Bahrani S, Vijayakameswara Rao N, et al. Bioactive graphene quantum dots-based polymer composite for biomedical applications. *Polymers (Basel)* **2022**; 14: 617. doi: 10.3390/polym14030617.
8. Chen D, Liu X, Lu X, Tian J. Nanoparticle drug delivery systems for synergistic delivery of tumor therapy. *Front Pharmacol* **2023**; 14: 1111991. doi: 10.3389/fphar.2023.1111991.
9. Emadi F, Emadi A, Gholami A. A comprehensive insight towards pharmaceutical aspects of graphene nanosheets. *Curr Pharm Biotechnol* **2020**; 21: 1016-27. doi: 10.2174/1389201021666200318131422.
10. Mousavi SM, Hashemi SA, Yari Kalashgrani M, Kurniawan D, Gholami A, Rahmanian V, et al. Recent advances in inflammatory diagnosis with graphene quantum dots enhanced SERS detection. *Biosensors (Basel)* **2022**; 12: 461. doi: 10.3390/bios12070461.
11. Gholami A, Emadi F, Amini A, Shokripour M, Chashmpoosh M, Omidifar N. Functionalization of graphene oxide nanosheets can reduce their cytotoxicity to dental pulp stem cells. *J Nanomater* **2020**; 2020: 6942707. doi: 10.1155/2020/6942707.
12. Gholami A, Emadi F, Nazem M, Aghayi R, Khalvati B, Amini A, et al. Expression of key apoptotic genes in hepatocellular carcinoma cell line treated with etoposide-loaded graphene oxide. *J Drug Deliv Sci Technol* **2020**; 57: 101725. doi: 10.1016/j.jddst.2020.101725.
13. Mousavi SM, Hashemi SA, Gholami A, Mazraedoost S, Chiang WH, Arjmand O, et al. Precise blood glucose sensing by nitrogen-doped graphene quantum dots for tight control of diabetes. *J Sens* **2021**; 2021: 5580203. doi: 10.1155/2021/5580203.
14. Mousavi SM, Hashemi SA, Yari Kalashgrani M, Gholami A, Binazadeh M, Chiang WH, et al. Recent advances in energy storage with graphene oxide for supercapacitor technology. *Sustain Energy Fuels* **2023**; 7: 5176-97. doi: 10.1039/d3se00867c.
15. Hu N, Zhu A, Si Y, Yue J, Wang X, Wang J, et al. A phase II, single-arm study of apatinib and oral etoposide in heavily pre-treated metastatic breast cancer. *Front Oncol* **2020**; 10: 565384. doi: 10.3389/fonc.2020.565384.
16. Yaghoubi F, Hosseini Motlagh NS, Naghib SM, Haghiralsadat F, Zarei Jaliani H, Moradi A. A functionalized graphene oxide with improved cytocompatibility for stimuli-responsive co-delivery of curcumin and doxorubicin in cancer treatment. *Sci Rep* **2022**; 12: 1959. doi: 10.1038/s41598-022-05793-9.
17. Yanikoglu R, Karakas CY, Ciftci F, Insel MA, Karavelioglu Z, Varol R, et al. Development of graphene oxide-based anticancer drug combination functionalized with folic acid as nanocarrier for targeted delivery of methotrexate. *Pharmaceutics* **2024**; 16: 837. doi: 10.3390/pharmaceutics16060837.
18. Rajaei M, Rashedi H, Yazdian F, Navaei-Nigjeh M, Rahdar A, Díez-Pascual AM. Chitosan/agarose/graphene oxide nanohydrogel as drug delivery system of 5-fluorouracil in breast cancer therapy. *J Drug Deliv Sci Technol* **2023**; 82: 104307. doi: 10.1016/j.jddst.2023.104307.
19. Marcano DC, Kosynkin DV, Berlin JM, Sinitskii A, Sun Z, Slesarev AS, et al. Correction to improved synthesis of graphene oxide. *ACS Nano* **2018**; 12: 2078. doi: 10.1021/acsnano.8b00128.
20. Sabzevari M, Cree DE, Wilson LD. Graphene oxide-chitosan composite material for treatment of a model dye effluent. *ACS Omega* **2018**; 3: 13045-54. doi: 10.1021/acsomega.8b01871.
21. Mohkam M, Rasoul-Amini S, Shokri D, Berenjian A, Rahimi F, Sadraeian M, et al. Characterization and in vitro probiotic assessment of potential indigenous *Bacillus* strains isolated from soil rhizosphere. *Minerva Biotecnol* **2016**; 28: 19-28.
22. Mohkam M, Nezafat N, Berenjian A, Zamani M, Dabbagh F, Bigharaz R, et al. Multifaceted toxin profile of *Bacillus* probiotic in newly isolated *Bacillus* spp. from soil rhizosphere. *Biologia* **2020**; 75: 309-15. doi: 10.2478/s11756-019-00357-1.
23. Alfandari J, Shnitman Magal S, Jackman A, Schlegel R, Gonen P, Sherman L. HPV16 E6 oncoprotein inhibits apoptosis induced during serum-calcium differentiation of foreskin human keratinocytes. *Virology* **1999**; 257: 383-96. doi: 10.1006/viro.1999.9675.
24. Srivastava N, Saxena A, Saxena AK. Small molecules as immune checkpoint inhibitors in cancer therapeutics. *Oncol Adv* **2024**; 2: 148-57. doi: 10.14218/OnA.2024.00019.
25. Liu B, Zhou H, Tan L, Siu KT, Guan XY. Exploring treatment options in cancer: tumor treatment strategies. *Signal Transduct Target Ther* **2024**; 9: 175. doi: 10.1038/s41392-024-01856-7.
26. Lee J, Choi MK, Song IS. Recent advances in doxorubicin formulation to enhance pharmacokinetics and tumor targeting. *Pharmaceuticals (Basel)* **2023**; 16: 802. doi: 10.3390/ph16060802.
27. Gabizon AA, Gabizon-Peretz S, Modaresahmadi S, La-Beck NM. Thirty years from FDA approval of pegylated liposomal doxorubicin (Doxil/Caelyx): an updated analysis and future perspective. *BMJ Oncol* **2025**; 4: e000573. doi: 10.1136/bmjonc-2024-000573.
28. Asgari S, Pourjavadi A, Setayeshmehr M, Boisen A, Ajalloueian F. Encapsulation of drug-loaded graphene oxide-based nanocarrier into electrospun pullulan nanofibers for potential local chemotherapy of breast cancer. *Macromol Chem Phys* **2021**; 222: 2100096. doi: 10.1002/macp.202100096.
29. Geyik G, Güncüm E, Işıklan N. Design and development of pH-responsive alginate-based nanogel carriers for etoposide delivery. *Int J Biol Macromol* **2023**; 250: 126242. doi: 10.1016/j.ijbiomac.2023.126242.
30. Alsalhi A, Ayon NJ, Coulibaly F, Alshamrani M, Al-Nafisah A, Youan BC. Enhancing etoposide aqueous solubility and anticancer activity with L-arginine. *Assay Drug Dev Technol* **2021**; 19: 508-25. doi: 10.1089/adt.2021.085.
31. Rahdar A, Sayyadi K, Sayyadi J, Yaghobi Z. Nano-gels: a versatile nano-carrier platform for drug delivery systems: A mini review. *Nanomed Res J* **2019**; 4: 1-9. doi: 10.22034/nmrj.2019.01.001.
32. Sharifian Dastjerdi Z, Kargar Abargouei E, Jafari S, Eftekhar E, Pourentezari M, Zamani Rarani F, et al. Evaluation of lomustine-loaded iron nanoparticles on caspase-6 gene expression and cell viability in U87Mg cell line. *Int Electron J Med* **2020**; 9: 124-9. doi: 10.34172/iejm.2020.23.
33. Guliyeva NA, Abaszade RG, Khanmammadova EA, Azizov EM. Synthesis and analysis of nanostructured graphene oxide. *J Optoelectron Biomed Mater* **2023**; 15: 23-30. doi: 10.15251/jobm.2023.151.23.
34. Qiao H, Chen X, Chen E, Zhang J, Huang D, Yang D, et al. Folated pH-degradable nanogels for the simultaneous delivery of docetaxel and an IDO1-inhibitor in enhancing cancer chemo-immunotherapy. *Biomater Sci* **2019**; 7: 2749-58. doi: 10.1039/c9bm00324j.
35. Mustafa A, Indiran MA, Ramalingam K, Perumal E, Shanmugham R, Karobari MI. Anticancer potential of thiocolchicoside and lauric acid loaded chitosan nanogel against oral cancer cell lines: a comprehensive study. *Sci Rep* **2024**; 14: 9270. doi: 10.1038/s41598-024-60046-1.
36. Taheriazam A, Gholamiyan Yousef Abad G, Hajimazdarany S, Imani MH, Ziaolhagh S, Zandieh MA, et al. Graphene oxide nanoarchitectures in cancer biology: nano-modulators of autophagy and apoptosis. *J Control Release* **2023**; 354: 503-22. doi: 10.1016/j.jconrel.2023.01.028.
37. Herdiana Y, Wathoni N, Gozali D, Shamsuddin S, Muchtaridi M. Chitosan-based nano-smart drug delivery system in breast cancer therapy. *Pharmaceutics* **2023**; 15: 879. doi: 10.3390/pharmaceutics15030879.
38. Jiang K, Wang Q, Chen XL, Wang X, Gu X, Feng S, et al. Nanodelivery optimization of IDO1 inhibitors in tumor immunotherapy: challenges and strategies. *Int J Nanomedicine* **2024**; 19: 8847-82. doi: 10.2147/ijn.S458086.

39. Mauri E, Giannitelli SM, Trombetta M, Rainer A. Synthesis of nanogels: current trends and future outlook. ***Gels*** 2021; 7: 36. doi: 10.3390/gels7020036.
40. Dabrowski B, Ulanowicz G, Brzozka Z, Zuchowska A. Studies of the interaction of graphene oxide (GO) with endothelial cells under static and flow conditions. *Environ Toxicol Pharmacol* **2024**; 110: 104541. doi: 10.1016/j.etap.2024.104541.
41. Azadi S, Osanloo M, Zarenezhad E, Farjam M, Jalali A, Ghanbariasad A. Nano-scaled emulsion and nanogel containing *Mentha pulegium* essential oil: cytotoxicity on human melanoma cells and effects on apoptosis regulator genes. *BMC Complement Med Ther* **2023**; 23: 6. doi: 10.1186/s12906-023-03834-y.
42. Adhikari HS, Yadav PN. Anticancer activity of chitosan, chitosan derivatives, and their mechanism of action. *Int J Biomater* **2018**; 2018: 2952085. doi: 10.1155/2018/2952085.
43. Fathima E, Nallamuthu I, Anand T, Naika M, Khanum F. Enhanced cellular uptake, transport and oral bioavailability of optimized folic acid-loaded chitosan nanoparticles. *Int J Biol Macromol* **2022**; 208: 596-610. doi: 10.1016/j.ijbiomac.2022.03.042.
44. Alkhatib MH, Al-Hashemi SM, Gashlan HM. Formulating etoposide in a nanoemulsion containing polyunsaturated fatty acids potentiates its anti-proliferation and anti-invasion activities against the ovarian cancer cells. *Biocell* **2021**; 45: 695-703. doi: 10.32604/biocell.2021.014349.
45. Liu J, Cui L, Losic D. Graphene and graphene oxide as new nanocarriers for drug delivery applications. *Acta Biomater* **2013**; 9: 9243-57. doi: 10.1016/j.actbio.2013.08.016.
46. Güncüm E, Geyik G, Işıklan N. Magnetic graphene oxide functionalized alginate-g-poly(2-hydroxypropylmethacrylamide) nanoplatform for near-infrared light/pH/magnetic field-sensitive drug release and chemo/phototherapy. *Int J Pharm* **2024**; 659: 124287. doi: 10.1016/j.ijpharm.2024.124287.
47. Wu S, Zhao X, Cui Z, Zhao C, Wang Y, Du L, et al. Cytotoxicity of graphene oxide and graphene oxide loaded with doxorubicin on human multiple myeloma cells. *Int J Nanomedicine* **2014**; 9: 1413-21. doi: 10.2147/ijn.S57946.
48. He P, Zou M, Zhang C, Shi Y, Qin L. Celastrol-loaded hyaluronic acid/cancer cell membrane lipid nanoparticles for targeted hepatocellular carcinoma prevention. *Cells* **2024**; 13: 1819. doi: 10.3390/cells13211819.
49. Bao J, Jiang Z, Ding W, Cao Y, Yang L, Liu J. Silver nanoparticles induce mitochondria-dependent apoptosis and late non-canonical autophagy in HT-29 colon cancer cells. *Nanotechnol Rev* **2022**; 11: 1911-26. doi: 10.1515/ntrev-2022-0114.
50. Aamazadeh F, Ostadrahimi A, Rahbar Saadat Y, Barar J. Bitter apricot ethanolic extract induces apoptosis through increasing expression of Bax/Bcl-2 ratio and caspase-3 in PANC-1 pancreatic cancer cells. *Mol Biol Rep* **2020**; 47: 1895-904. doi: 10.1007/s11033-020-05286-w.
51. Diepstraten ST, Anderson MA, Czabotar PE, Lessene G, Strasser A, Kelly GL. The manipulation of apoptosis for cancer therapy using BH3-mimetic drugs. *Nat Rev Cancer* **2022**; 22: 45-64. doi: 10.1038/s41568-021-00407-4.
52. Mousavi SM, Hashemi SA, Ghahramani Y, Azhdari R, Yousefi K, Gholami A, et al. Antiproliferative and apoptotic effects of graphene oxide @AlFu MOF based saponin natural product on OSCC line. *Pharmaceuticals (Basel)* **2022**; 15: 1137. doi: 10.3390/ph15091137.